DROPLET EVAPORATION TIME IN FILM BOILING REGION

M. Mousa

Mechanical Power Engineering Department, Faculty of Engineering,
Menoufia University, Shebin El-Kom, Egypt.

ABSTRACT

A closed correlation for vaporization time of discrete liquid droplet in film boiling region has been derived analytically and verified with experimental data. The heat conduction through the vapor layer to a single droplet in spheroid with flat bottom is performed. First, we deduced analytically an expression for the thickness of vapor layer under the droplet by solving the equations of momentum, energy balance at interface and balance of static forces exerting on the droplet simultaneously. Then the rate of droplet diameter decrement and evaporation time estimated by using the energy balance considering the heat required of complete evaporation equivalent heat conduction to the droplet. The droplet liquid includes water and various pure hydrocarbon fuels such as heptane, decane and hexadecane with droplet sizes ranging from 0.05 to 2 mm. The temperature of hot wall varying from 80 to 500 °C cover the heat transfer characteristics of nucleate, transition and film boiling regions. The maximum evaporation rate of the liquid droplet occurs at 30 - 60 °C above the boiling temperature for water and pure fuels. Also, the minimum evaporation rate (Leidenfrost temperature) occurs at 160 °C above boiling temperature for water and 70 - 90 °C above the boiling temperature for heptane, decane and hexadecane. The procedure we proposed predicts the droplet vaporization time in film boiling region fairly well.

Keywords: Leidenfrost Temperature, Droplet Evaporation, Droplet Diameter Decrement, Evaporation Heat Transfer, Film Boiling Region.

INTRODUCTION

Droplet impact cooling is a promising technology with potential applications in high-power solid state electronics, materials processing, aerospace flight, and energy conversion. Droplet evaporation upon heated surface at temperature above boiling point involves heat transfer in different modes. An important aspect in calculating the rate of heat released from a heated metal surface is to account of the heat transfer to a single droplet during the cooling process. In spray cooling process of heated surface, the heat transfer characteristics have three distinctive regions according to the surface temperature, that is the regions associated with nucleate, transition and film boiling [1-3]. Most previous Investigators studied the mechanism of heat transfer between heated metal surface and liquid droplet as two parallel conductances. The vapor outguessing beneath a droplet in film boiling region is assumed to resemble fully developed laminar flow between parallel plates. Baumeister *et al.* [4-6] studied theoretically and experimentally the mass evaporation rates and overall heat transfer coefficient for water droplet which are supported by their own superheated vapor upon a flat heated plate. The water droplet in film boiling region is assumed to have a flat disk geometry with a uniform vapor gap between the droplet, forming an insulating layer between the droplet and heated surface [7-8]. Baumeister *et al.* [6] have summarized the relation between the shape and the dimensionless volume of droplet in film boiling region and reviewed in the previous report [1]. For small droplet, $d_o \leq 3$ (mm), the

dimensionless volume $V^* \leq 0.8$ and dimensionless bottom area $A^* = 1.81V^*$ is rearranged in dimensional form. The radius of the flat bottom as a function of the initial droplet diameter is obtained as $r_b = 0.612\, d_o$. The comparison between Baumeister's correlation and experimental data are made. Many discrepancies for droplet vaporization time and heat flux are found between the prediction and the experimental data especially for small droplets.

Emmerson [9] studied experimentally the effect of surface material and pressure on evaporation time of discrete droplet in film boiling region. Much attention was made to the wettability and thermal diffusivity of surface as to heat transfer characteristics. The evaporation time is reduced as the pressure is increased, and Leidenfrost temperature increases with pressure. The Leidenfrost temperature varies with pressure in a way peculiar to any given material of heating surface and no single correlation with pressure can embrace all surface materials whatever their roughness. The evaporation characteristics of water in fuel emulsion droplets in film boiling on a heated surface are studied experimentally [10,11]. Preferential vaporization of either fuel or water can occur from an evaporating water-in-fuel emulsion droplet. For heptane water emulsions, heptane was preferentially evaporated from the droplets, whereas for water decane emulsions, water prevaporization occurs before decane. The results also show that the droplet evaporation rate decreases, and the total droplet evaporation time increases with increasing water content. The maximum heat transfer rate occurs at 50 ~ 60 °C above the boiling temperature for all pure liquids and the Leidenfrost heat transfer rate (beginning of film boiling region) occurs at about 120 °C for pure fuel and 180 °C for water above boiling temperature at atmospheric pressure. The maximum evaporation rate can significantly exceed the burning rate for fuel droplet [11]. The droplet evaporation and the heat transfer rate from the heated surface in nucleate and transition boiling regions have been investigated experimentally [12]. Efforts are focused on the use of much larger liquid droplets in the cooling system to demonstrates the possibility of obtaining sustained, reasonably high heat fluxes with thicker films at moderates surface superheating. Li *et al.* [13] studied the combustion characteristics and burning rate of four energetic fuel droplets. They concluded that the high-energy-density fuel does not automatically imply that it is fast burning, and that it must also possess desirable combustion characteristics, especially minimal sooting formation, before it can be considered for use as a jet fuel.

The objective of the present study is to develop a closed correlation for vaporization time of small droplet in film boiling region. Also modify the thickness of vapor layer under the droplet and heated surface as a function of droplet diameter, surface temperature, liquid hydrodynamic variables and the vapor thermal properties. Both the validity and limitation of correlation are experimentally examined at various liquid droplet sizes and surface superheating.

HEAT TRANSFER ANALYSIS OF SINGLE DROPLET

Model of Droplet Evaporation

The heat transfer analysis of single droplet in film boiling region is based on the model shown in Figure 1. The droplet is nearly spherical and floating on the heat transfer surface in spheroid upon couch of vapor layer. A thin vapor layer insulates the lower face of the droplet with minimum thickness and the heat is transferred by conduction through this vapor layer.

The following assumptions are made.

1. No evaporation takes place before the droplet reaches the surface.
2. The time necessary for starting evaporation and changing shape from spherical to spheroid is negligible in comparison with the total lifetime of droplet.
3. The direct contact heat transfer between liquid and heat transfer surface is negligible.
4. The radiation heat transfer from the heating surface to the lower and upper faces of the droplet and mass diffusion

from droplet are small compared with evaporation rate through the vapor layer under the droplet.

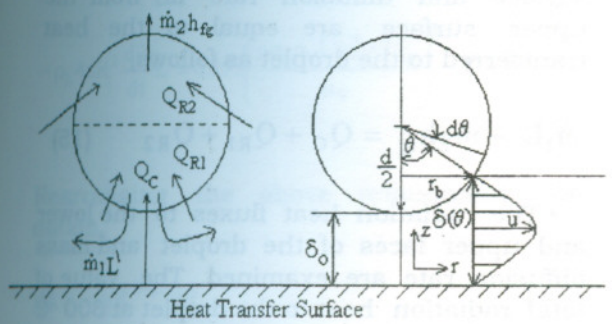

Figure 1 Model of droplet evaporation in film boiling region.

The geometric relationships of droplet in spherical shape are

$$\delta(\theta) = \delta_o + \frac{d}{2}(1-\cos\theta)$$
$$r = \frac{d}{2}\sin\theta, \qquad dr = \frac{d}{2}\cos\theta\, d\theta \tag{1}$$

The heat transferred to the droplet by conduction through the vapor layer under the droplet as follows:

$$q_C = \int_{Ap} \frac{k_v}{\delta(\theta)}(T_w - T_S) = \frac{kv}{\delta m}(T_w - T_S) \tag{2}$$

Where, the average thickness of vapor layer under the droplet defined as,

$$\delta_m = \frac{1}{\theta}\int_0^\theta \delta(\theta)d\theta = \frac{1}{\theta}\int_0^\theta \left(\delta_o + \frac{d}{2}(1-\cos\theta)\right)d\theta \tag{3}$$

The integration of the above relation from θ = 0 to $\pi/2$ yields,

$$\delta_m = \frac{2}{\pi}\left[\delta_o\theta + \frac{d}{2}(\theta - \sin\theta)\right]_0^{\frac{\pi}{2}}$$
$$\delta_m = \delta_o + \frac{d}{2}\left(\frac{\pi-2}{\pi}\right) \tag{4}$$

The radius of projection segment area (bottom contact area) which heat is transferred by conduction is,

$$r_b = \sqrt{\left(\frac{d}{2}\right)^2 - \left(\frac{d}{2}\right)^2\left(\frac{\pi-2}{\pi}\right)^2} = 0.466d \tag{5}$$

The droplet shape can be simplified to spheroid with flat bottom as shown in Figure 2.

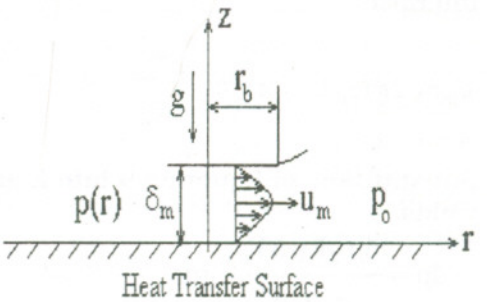

Figure 2 Droplet evaporation in spheroid with flat bottom.

The momentum balance considering to the vapor layer under the droplet with constant thickness as [7, 8],

$$\frac{dp}{dr} = \mu_V \frac{\partial^2 u}{\partial z^2} \tag{6}$$

The boundary conditions for vapor radial velocity, temperature and pressure under the droplet are

u=0	at	z=0, δ_m	
P=p_o	at	$r=r_b$, $0 \le z \le \delta_m$	(7)
T=f(z) = T_w	at	z=0	
T=f(z)=T_S	at	$z=\delta_m$	

Equation 6 may be integrated assuming no slip at the vapor boundaries Equation [7] to

$$u = \frac{1}{2\mu_V}\frac{dp}{dr}\left(z^2 - z\delta_m\right) \tag{8}$$

The average radial velocity of the vapor underneath the droplet is, (9)

$$u_m = \frac{1}{\delta_m}\int_0^{\delta_m} u\,dz$$

$$u_m = \frac{\delta_m^2}{12\mu_V}\left(-\frac{dp}{dr}\right) \qquad (9)$$

For small cylinder with radius r and height δ_m, the evaporation rate is equal to the heat conduction through vapor layer under the droplet, (energy balance at interface)

$$u_m \rho_V 2\pi r \delta_m L' = \pi r^2 k_V \frac{\Delta T_{sup}}{\delta_m} \qquad (10)$$

Substitution of Equation 9 into Equation 10 yields,

$$-dp = \frac{6\mu_V k_V \Delta T_{sup}}{\rho_V L' \delta_m^4} r\,dr \qquad (11)$$

The integration using boundaries Equation 7 giving the pressure distribution as,

$$p - p_o = \frac{3\mu_V k_V \Delta T_{sup} r_b^2}{\rho_V L' \delta_m^4} \qquad (12)$$

The static balance of forces upon the droplet yields,

$$\int_0^{r_b} 2\pi r(p - p_o)dr = \frac{\pi}{6}\rho_L d^3 g$$

$$\frac{6\pi\mu_V k_V \Delta T_{sup} r_b^2}{\rho_V L' \delta_m^4}\int_0^{r_b} r\,dr = \frac{\pi}{6}\rho_L d^3 g \qquad (13)$$

With integrating the above equation, we obtains the thickness of the vapor layer under the droplet as,

$$\delta_m = \left(\frac{18\mu_V k_V \Delta T_{sup} r_b^4}{g\rho_L \rho_V L' d^3}\right)^{0.25} \qquad (14)$$

The droplet energy balance involves, Q_C, the heat conduction from the vapor layer, Q_{R1}, the radiation heat to the lower surface and, Q_{R2}, the radiation heat to the upper surface. The evaporation rate m_1 from the lower surface and diffusion rate m_2 from the upper surface are equal to the heat transferred to the droplet as follows,

$$\dot{m}_1 L' + \dot{m}_2 h_{fg} = Q_C + Q_{R1} + Q_{R2} \qquad (15)$$

• The radiation heat fluxes to the lower and upper faces of the droplet and mass diffusion rate are examined. The value of total radiation heat to the droplet at 300 °C is found about 5.4 % of evaporation heat and the diffusion heat may less than 1 %. So the contribution of radiation and diffusion heat are neglected in this study. Thereafter, the heat transferred from the heated surface through the vapor layer causes the evaporation rate and decreases the droplet radius. Setting $r_b = 0.466d$ in Equation 10 and Equation 14 yields the heat transfer rate to the droplet. The energy balance of a small droplet at the interface is given by

$$-\rho_L \frac{dV}{d\tau} L' = C_f \pi r_b^2 k_V \left(\frac{\Delta T_{sup}}{\delta_m}\right) \qquad (16)$$

Where, C_f = 0.41 is the area correction factor and defined as the ratio between the flat bottom area and the lower face of the droplet. After rearranging, Equation 16 yields,

$$-\rho_L \frac{dV}{d\tau} L' = 0.292\left(\frac{g\rho_L \rho_V d^7 L' k_V^3 \Delta T_{sup}^3}{\mu_V}\right)^{0.25} \qquad (17)$$

Where, L' is the vaporization heat, which the vapor in the film between droplet and heated surface is assumed superheated to a temperature halfway between saturation temperature and surface temperature,

$$L' = C_{P_L}(T_S - T_L) + h_{fg} + C_{P_V}(T_V - T_S) \qquad (18)$$

Substituting Equation 15 into Equation 17, we obtain a relationship between time decrement and droplet radius as follows,

$$-\rho_L 4\pi R^2 \frac{dR}{d\tau} L' = 0.292 \left(\frac{g\rho_L \rho_V L' k_V^3 \Delta T_{sup}^3}{\mu_V} \right)^{0.25} (2R)^{1.75} \quad (19)$$

Rearranging the above relationship, we obtain,

$$d\tau = -\psi R^{0.25} dR \quad (20)$$

Where,

$$\psi = 2.155 \left(\frac{\mu_V \rho_L^3 L'^3}{g\rho_V k_V^3 \Delta T_{sup}^3} \right)^{0.25} \quad (21)$$

The integration of Equation 20 for small interval time gives the change of droplet radius as,

$$\Delta\tau = -\frac{\psi}{1.25} \left(R_2^{1.25} - R_1^{1.25} \right) \quad (22)$$

Also the integration of Equation 20 from initial droplet radius, R_o, until the droplet disappears (complete evaporation) yields the vaporization time. So the vaporization time of small droplet in film boiling region is derived as,

$$\tau_{ev} = 0.725 \left(\frac{\mu_V \rho_L^3 L'^3 d_o^5}{g\rho_V k_V^3 \Delta T_{sup}^3} \right)^{0.25} \quad (23)$$

The droplet radius decrement with time and total vaporization time can be calculated theoretically from Equations 22 and 23. The droplet radius decrement and total vaporization time are very sensitive to surface temperature, surface material, vapor and liquid properties. In the nucleate boiling region, the droplet spreads upon the surface forming liquid film which wetted the heat transfer surface, and takes very short time for complete evaporation *(direct contact heat transfer)*. In the transition region, unstable thin vapor layer exists under the droplet, and the droplet shrinks to spheroid shape. In film boiling region, the vapor layer becomes stable and isolates the droplet bottom area from the heat transfer surface. With increasing the surface temperature, the droplet shrinks more until becomes nearly spherical except the bottom contact area and the droplet vaporization time becomes large. The correlation of vaporization time, Equation 23, must still be validated by means of a comparison with experimental results.

RESULTS AND DISCUSSIONS

Comparison between Theoretical Model and Experiments

Such a comparison is shown in Figure 3 for results related to water, decane, hexadecane and heptane data. As seen in Figure 3, the correlation of droplet vaporization time in film boiling region, (Equation 23), reproduce well the experimental data [10, 11] for various liquids at certain droplet sizes. It was found that the available experimental water data are predicted with an accuracy of less than ±2% for droplet size less than 1 mm and ±15% for droplet size from 1 to 2 mm. The comparison is very closed between prediction by the proposed model and experiments for decane data with droplet size less than 0.5 mm. Also for hexadecane and heptane data, the prediction is very closed to experiments for small droplet size less than 0.5 mm with an accuracy of less than ±20%, and such an agreement confirms the validity of the proposed model.

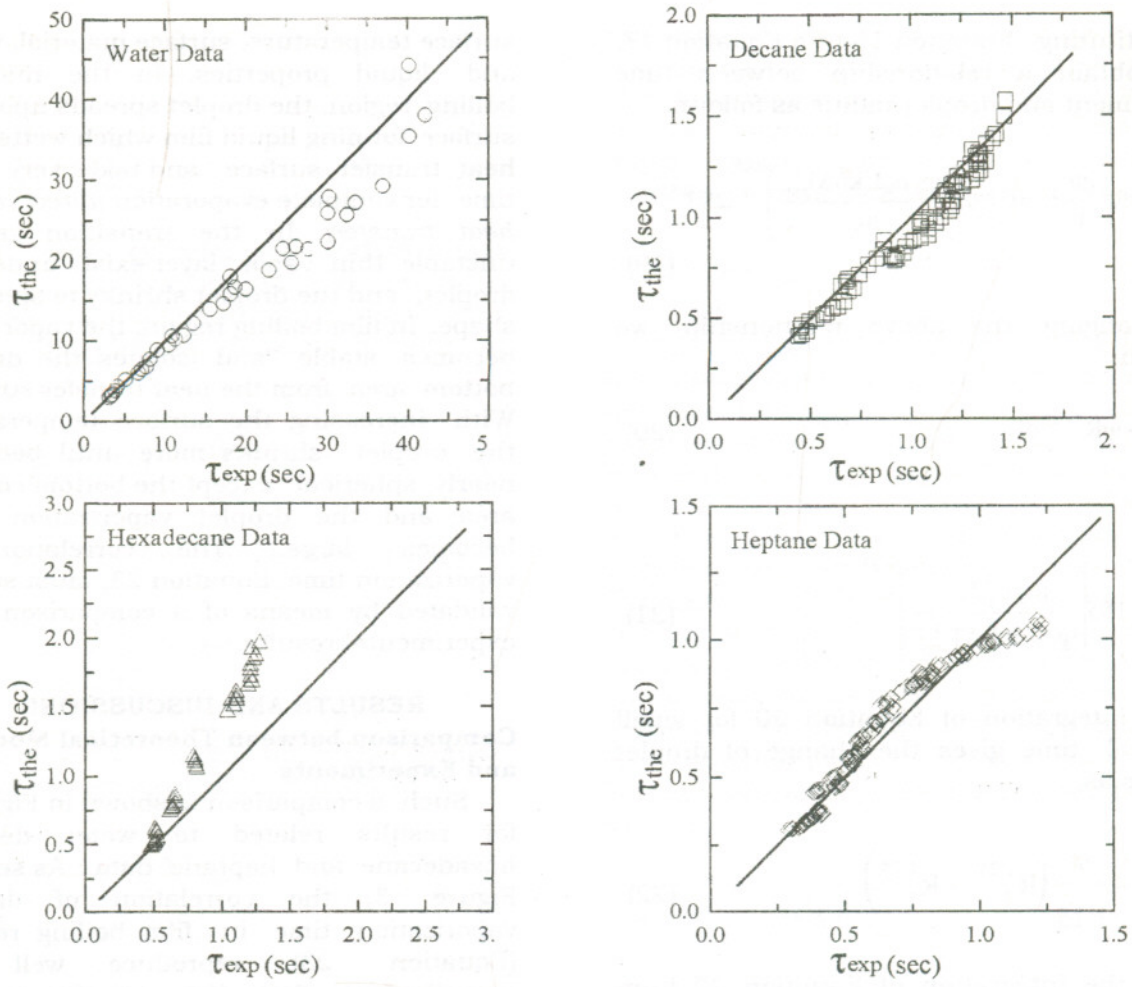

Figure 3 Comparison between prediction and experimental data for droplet evaporation time.

Temporal Variation of Droplet Diameter

Table 1 shows the comparison between the experimental data of vaporization time at certain surface temperature and droplet diameter [10], and the prediction by correlation of τ_{ev}. For water, the average deviation between experimental and calculated data is ±6%, but for heptane and decane data are ±4.53% and ±11.7% respectively. The effect of droplet size and surface temperature on the evaporation time of Equation 22 is shown in Figures 4 to 6. The vaporization time decreases with increasing surface superheating and increased with increasing droplet size. It is evident that the contact area between the droplet and hot surface has decreased as the vaporization time also decreased. The variation of droplet diameter throughout the vaporization time has been examined by Equations 20 to 22 and compared with experimental data. For the water data in Figure 4, the predicted qualitative trends for the variation of droplet size show the best agreement with experimental data. For heptane data presented in Figure 5, the prediction is very satisfactory, but for decane data, which illustrated in Figure 6, some discrepancies were obtained especially at the end of vaporization time upon the heated surface. The discrepancy between prediction and experiment for decane data may be due to the effect of droplet explosion at the end of vaporization time and droplet

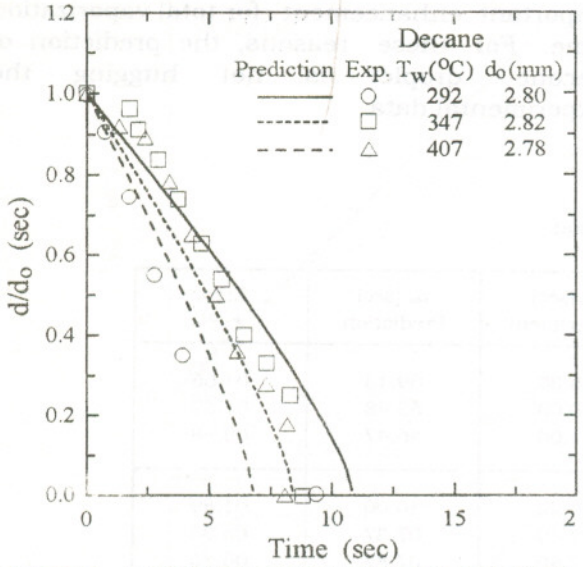

Figure 6 Comparison between prediction and experimental data for decane droplet decrement.

Total Vaporization Time in Spheroid State

Figures 7 to 9 show typical experimental data for vaporization time of water, hexadecane and heptane as a function of surface temperature, droplet size and hydrodynamic properties of vapor and liquid [11]. The comparison between prediction by Equation 23 and experimental data is fairly well for small droplet size. For water data as shown in Figure 7, at large droplet from 1 ~ 2 mm, the prediction results are less than the experiments because the droplet may not in spheroid state and the explosion of the vapor layer under the droplet is occurred. Figures 8 and 9 show the prediction by Equation 23 and experimental data of hexadecane and heptane. Qualitatively the shapes of the prediction curves are not similar to the experiment because the rapid local boiling at the liquid-solid interfaces which causes droplet distortion and ultimately disintegration. The result of the disintegration of droplet is almost instantaneous evaporation and the slope of curves is not the same. The effect of droplet size and type of fuel on vaporization time are illustrated in Figures. 8 and 9. The vaporization time decreased in film boiling region with increasing surface superheating. This is to be expected because the contribution of radiation heat increases with increasing surface superheating. Also, the density and thermal properties of vapor are varying with increasing surface superheating above boiling temperature.

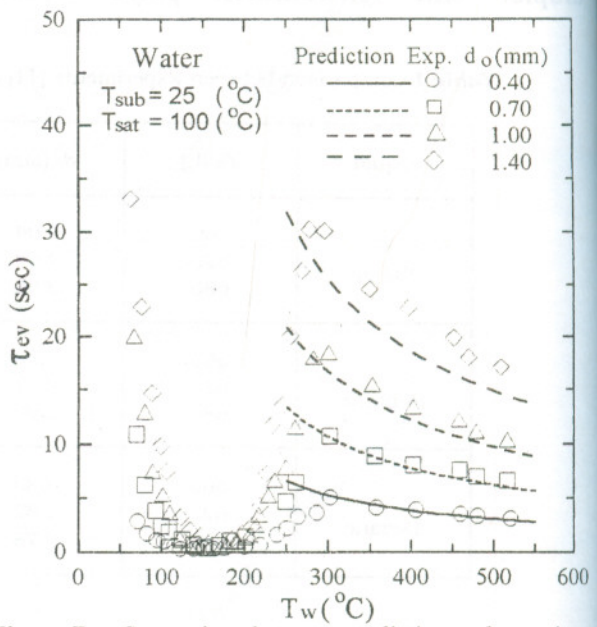

Figure 7 Comparison between prediction and experimental data for water droplet evaporation time.

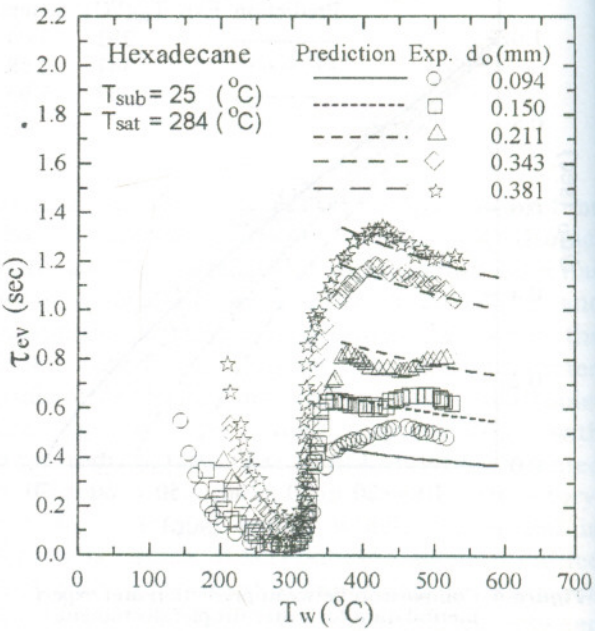

Figure 8 Comparison between prediction and experimental data for hexadecane droplet evaporation time.

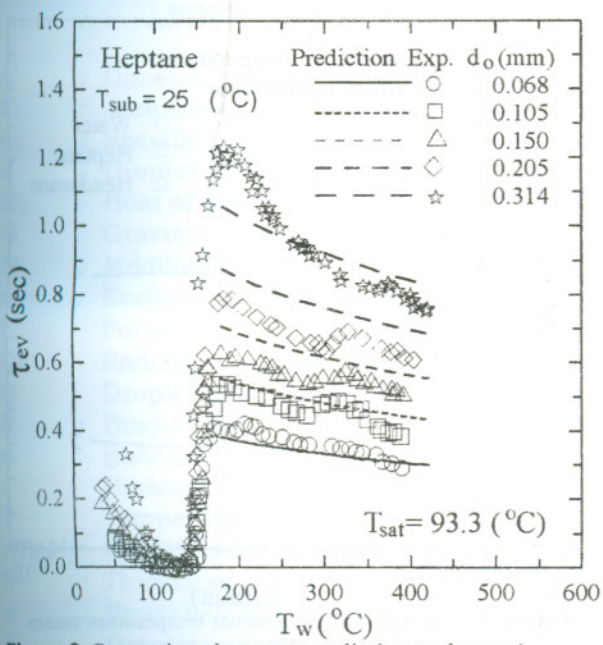

Figure 9 Comparison between prediction and experimental data of heptane droplet evaporation time.

Droplet Heat Transfer Rate

In the present work, the average heat transfer rate from the heated surface to the droplet in spheroid shape can be expressed as,

$$q = \frac{\pi \rho_L d_o^3 L}{6 \tau_{ev}} \qquad (24)$$

Figures 10 to 12 show the dependence of heat transfer rate, q, on the surface superheating and initial droplet size for water, hexadecane and heptane. Similar to the conventional trend of pool boiling curve, the data demonstrate three distinctive regions can be recognized, namely, the region associated with nucleate, transition and film boiling. At minimum vaporization time, the droplet takes very short time for complete evaporation and the heat transfer rate reaches maximum at surface temperature 50 ~ 60 °C above boiling temperature for water and 20 ~ 40 °C for hexadecane and heptane as shown in Figure 13. Also as is shown, the heat transfer rate attained the minimum at Leidenfrost temperature of 160 ~ 180 °C above boiling temperature for water and 70 ~ 90 °C for hexadecane and heptane. The maximum heat transfer rate to the droplet basically depends on the transient heating time of the droplet residing on the heated surface to be heated to the boiling temperature. Since the boiling temperature of hexadecane (284 °C) is much higher than heptane and water, therefore Leidenfrost temperature is also lower resulting in lower heat flux to the droplet at different size. For smaller droplets where droplets can bounce ten or more diameters from the surface, thus heat transfer rate increases with increasing droplet size. For hexadecane droplet, the Leidenfrost temperature is about 380 °C, that is much higher than heptane, which is at about 180 °C, therefore radiation heat transfer to hexadecane droplet is higher. So the surface superheating which the maximum and minimum heat transferred from the heated surface the heptane droplet is higher than hexadecane.

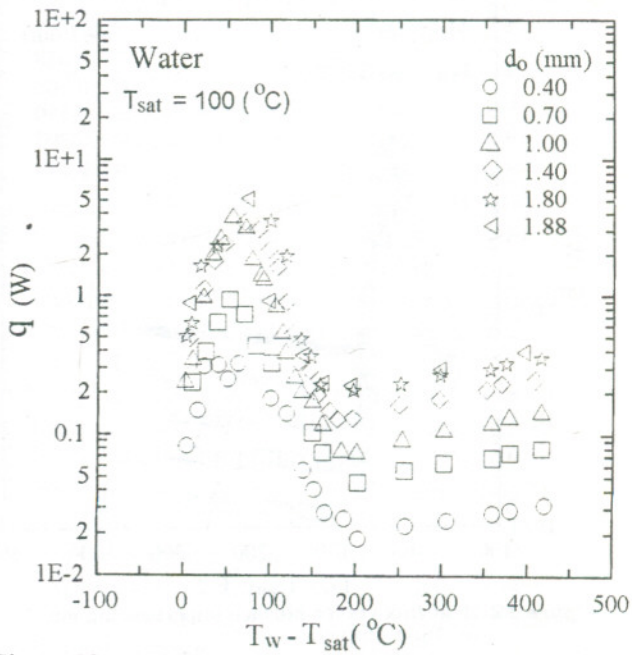

Figure 10 Heat flux verses surface superheating for water droplet.

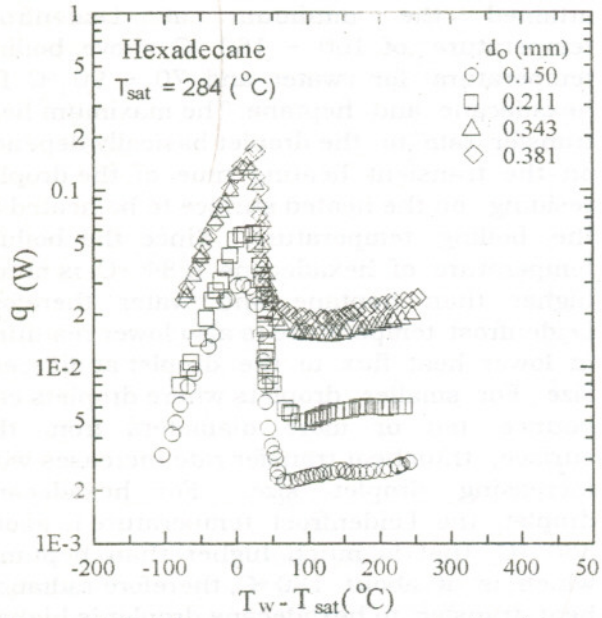

Figure 11 Heat flux verses surface superheating for hexadecane droplet.

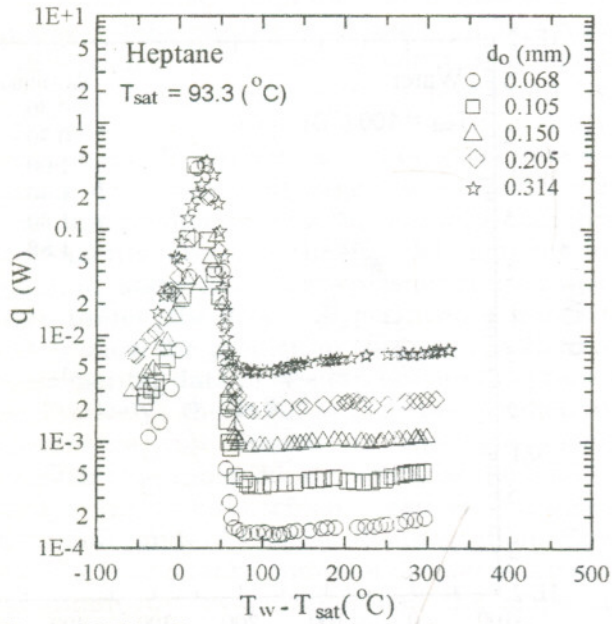

Figure 12 Heat flux verses surface superheating for heptane droplet.

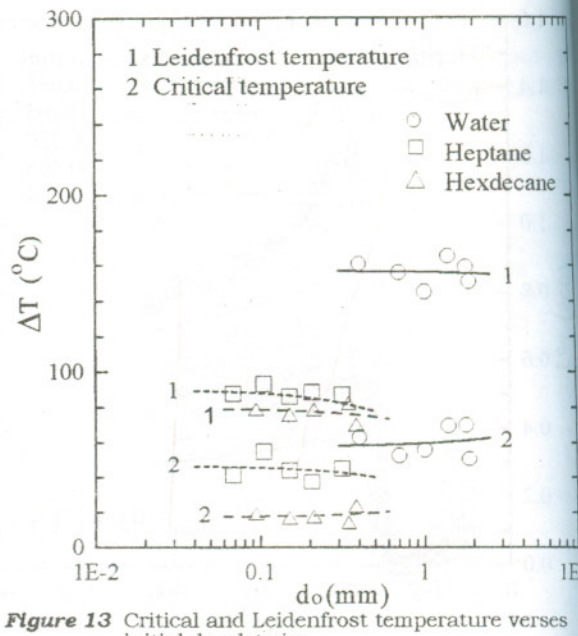

Figure 13 Critical and Leidenfrost temperature verses initial droplet size.

CONCLUSION

An analytical model has been developed to predict the droplet vaporization time in film boiling region that are supported by their own superheated vapor over a flat heated surface. The liquid droplet is assumed to be of a spheroid shape with a uniform vapor gap beneath the droplet and the droplet bottom is at saturation temperature. The evaporation takes place uniformly beneath the droplet. For steady-state laminar incompressible flow, the momentum equation with inertia terms neglected, the mass balance and the energy balance at interface are solved simultaneously to obtain the vaporization time of the droplet. The change of droplet diameter throughout evaporation is calculated and tested with the experimental data. The prediction is more satisfactory for water and heptane data but for decane data, some discrepancies were found. The droplet vaporization time is estimated by correlation of τ_{ev}, and the comparison between the experimental data and prediction is fairly well. The maximum heat transfer rate, which can significantly exceed the value of burning droplet occurs at 50 ~ 60 °C above the boiling temperature for water and 20 ~ 40 °C for fuels. The Leidenfrost heat transfer rate occurs at about 160 ~ 180 °C for water above the boiling temperature and 70 ~ 90 °C for fuels.

NOMENCLATURE

A'	:	Dimensionless bottom area [-]
C_f	:	Area correction factor [-]
C_p	:	Specific heat [j/(kg. K)
d	:	Droplet diameter [m]
h_{fg}	:	Heat of vaporization [j/kg]
G	:	Gravity acceler-ation [m/s^2]
L\	:	Modified latent heat [j/kg]
m	:	Evaporation rate [kg/s]
P		Pressure [N/m^2]
Q_R		Radiation heat transfer [W]
Q		Droplet heat flux [W]
R	:	Droplet radius [m]
r_b	:	Radius of droplet bottom [m]
r		Horizontal axis [m]
T		Temperature [°C]
ΔT_{sup}		Surface superheating, Tw-Ts, [K]
δ	:	Thickness of vapor layer [m]
u	:	Vapor velocity [m/s]
V		Droplet volume [m^3]
Z	:	Vertical axis [m]
κ	:	Thermal conductivity [W/(m. K)]
μ	:	Viscosity [Pa. s]
θ	:	Angle [°]
ρ	:	Density [kg/m^3]
τ		Time [s]
τ_{ev}		Vaporization time [s]

Subscripts

0 : Initial, environment
1 : Droplet lower face
2 : Droplet upper face
c : Conduction
L : Liquid
m: Mean
S : Saturation
V : Vapor
W: Wall

REFERENCES

1. T. Ito, Y. Takata and M. M. M. Mousa, "Studies on the Water Cooling of Hot Surfaces (Analysis of Spray Cooling in the Region Associated with Film Boiling)", JSME International Journal, Series II, Vol. 35, No. 4, pp. 589-598, (1992).
2. M.M. Mohamed Mousa, "Spray Cooling of Hot Surfaces", Ph. D. Thesis, Kyushu University, Faculty of Engineering, Fukuoka 812, Japan, (1992).
3. T. Ito, Y. Akata and M.M.M. Mousa H. Yoshikai, "Studies on the Water Cooling of Hot Surfaces (Experiment of Spray Cooling)", Memoirs of the Faculty of Eng., Kyushu Univ., Vol. 51, No. 2, pp.119-144, (1991).
4. K. J. Baumeister and T.D. Hamill, "Creeping Flow Solution of the Leidenfrost Phenomenon", NASA TND–3133, (1965).
5. K. J. Baumeister, R. C. Hendricks and T.D. Hamil, "Metastable Leidenfrost States", NASA TN – 3226, (1966).
6. K. J. Baumeister E.G. Keshock D. A. and Pucci, "Anomalous Behavior of Liquid Nitrogen Drops in Film Boiling", NASA TM X – 52800, (1970).
7. L. H. J. Watchters, H. Bionne and H. J. Van Nouhuis, "The Heat Transfer from a Hot Horizontal Plate to Sessile Water Drops in the Spheroidal State", Chem. Eng. Sci., Vol. 21, pp. 923-936, (1966).
8. B. S. Gottfried, C. J. Lee and K. J. Bell, "The Leidenfrost Phenomenon: Film Boiling of Liquid Droplets on a Flat plate", Int. J. Heat Mass Transfer, Vol. 9, pp. 1167-1187, (1966).
9. G. S. Emmerson, "The Effect of Pressure and Surface Material on the Leidenfrost Point of Discrete Drops of water", Int. J. Heat Mass Transfer, Vol. 18, pp. 381-386, (1975).
10. C. T. Avedisian and M. Fatehi, "An Experimental Study of the Leidenfrost Evaporation Characteristics of Emulsified Liquid Droplets", Int. J. Heat Mass Transfer, Vol. 31, No. 8, pp. 1587-1603, (1988).
11. T.Y. Xiong and M. C. Yuen, "Evaporation of a Liquid Droplet on a Hot Plate", Int. J. Heat

Mass Transfer, Vol. 34, No. 7, pp. 1881-1894, (1991).
12. P.J. Halvorson, R.J. Carson, S.M. Jeter and S.I. Abdel-Khalik, "Critical Heat Flux Limits for a Heated Surface Impacted by a Stream of Liquid Droplets", Journal of heat Transfer, ASME, Vol. 116, pp. 679-685, (1994).
13. T. X. Li, D.L. Zhu and C.K. Law, "Droplet Combustion, Microexplosion, and Sooting Characteristics of Several Energetic Liquid Propellants", Journal of Propulsion and Power, Vol. 14, No. 1, pp. 45-50, (1998).
14. Robert C. Reid, John M. Prausnitz and Bruce E. Poling, "The Properties of Gases and Liquids", Fourth Edition, McGraw-Hill Book Company, (1987).

Received September 20,1998
Accepted April 4,1999

زمن تبخر القطرة فى منطقة الغليان الرقائقى

موسى محمد محمد موسى
قسم هندسة القوى الميكانيكيه - جامعة المنوفيه

ملخص البحث

تم الحصول بالطرق التحليلية على معادلة لتبخير قطرة السائل فى منطقة الغليان الرقائقى وتم اختبارها بالنتائج العملية، والقطرة على شكل شبه كروى بمساحة اتصال مستوية بينها وبين السطح الساخن وقد اعتبر أن انتقال الحرارة بالتوصيل من السطح الساخن إلى القطرة خلال طبقة من البخار أسفل القطرة بسمك منتظم. أولا" تم بالاستنتاج التحليلى الحصول على سمك طبقة البخار تحت القطرة بحل معادلات الحركة والطاقة واتزان القوى المؤثر على القطرة بالتوالى، بعد ذلك تم حساب معدل تناقص قطر القطرة نتيجة التبخير بمعادلة الحرارة المنتقلة بالتوصيل عبر طبقة البخار والحرارة اللازمة لتبخير القطرة بالكامل، وقد تم اختبار تبخير قطرات من الماء والوقود الهيدروكربونى مثل الهبتان والديسان والهكساديسان بقطر يتراوح من ٠,٠٥ حتى ٢ مم ودرجة حرارة للسطح الساخن من ٨٠ حتى ٥٠٠ °م. وقد لوحظ من الحسابات أن أعلى معدل لتبخير القطرات يتم عند درجة حرارة من ٣٠ إلى ٦٠ °م فوق درجة الغليان للماء والوقود الهيدروكربونى ، وأن أقل معدل للتبخير يتم عند درجة حرارة ١٦٠ °م فوق درجة الغليان للماء ودرجة ٧٠ حتى ٩٠ °م للوقود الهيدروكربونى، وبوجه عام فإن النموذج الرياضى المقترح ومعادلة زمن تبخير القطرة فى منطقة الغليان الرقائقى يمكن استخدامها بدرجة مقبولة من الثقة.